Denitrogenation and desulfurization of model oil through adsorption process using one-pot synthesized reusable CYCU-3@Al2O3 composites

Hongchen Fu, Zareen Zuhra, Shafqat Ali, Yunshan Zhou*, Lijuan Zhang*, Xiaoya Duan, Zipeng Zhao
State Key Laboratory of Chemical Resource Engineering, College of Chemistry, Beijing University of Chemical Technology, Beijing, 100029, P. R. China. zhouys@mail.buct.edu.cn (Y. Zhou), ljzhang@mail.buct.edu.cn (L. Zhang)

Apparatus

FT-IR analyses were examined on a MAGNA-IR 750 (Nicolet) spectrophotometer by using a KBr pellet and wavenumber was adjusted from 400 to 4000 cm^{-1}. The powder X-ray diffractions of the composites were measured by using a Shimadzu D-6000 X-ray diffractometer along with Cu-Kα irradiation (λ = 1.5418 Å) as a source. The SEM and EDX measurement were conducted with a Zeiss Supra 55 scanning electron microscopy and energy dispersive X-ray spectroscopy, respectively. For the SEM images of Al_2O_3 and the CYCU-3@Al_2O_3 composites, they beads were cut into two pieces, and the SEM image were taken from the cross section. The ICP elemental analysis was analyzed by the Spectro Arcosepo of the German Spike analysis instruments. The BET analyses were collected on an ASAP-2020 (Micrometrics USA) equipment at 77 K and nitrogen atmosphere. The specific surface area (SBET) was measured from the linear isotherm part of the BET equation (P/P_0 = 0.05-0.3). The distribution in pore size was derived from the desorption branch of the N_2 isotherm through a combination of Dubinin-Radushkevich (DR) method (0.35 – 10 nm pore size distribution analysis) and Barrett-Joyner-Halenda (BJH) method (10 – 70 nm pore size distribution analysis). TG/DTA analysis was made on a Netzsch STA449 with a temperature rate of 10 °C min-1 in the temperature range of 25 to 800 °C under air flow. HR-TEM images were obtained by JEOL JEM 2100 with the acceleration voltage of 200 kV. The sulfur and nitrogen content was studied by Agilent 1100 Series HPLC with following specifications: column of C-18 with 4.6 mm in diameter and 150 mm in length and filter of 5 μm in diameter, 30℃ of column temperature. The initial mobile phase was composed of 90% methanol and 10% water while the gradient elution was done by using a 100% methanol for 10 min with its flow rate of 1.0 mL/min.

Synthesis of CYCU-3@Al_2O_3 composites

In fact, we synthesized a series of CYCU-3@Al_2O_3 with different mass ratio of added H_2SDC to γ-Al_2O_3 in the synthesis process of our experiments (the 5%, 10% and 20% meant the mass ratio of added H_2SDC to γ-Al_2O_3 in the synthesis), including CYCU-3@Al_2O_3 (30%) and CYCU-3@Al_2O_3 (40%). By measuring the loading amount of MOF on Al_2O_3 through elemental analysis, we found that when it was greater than 20%, the loading amount of CYCU-3 on the carrier remained almost unchanged (The elemental analysis date is as follows), meantime more CYCU-3 powders also formed in the reaction solution, which is not good in economic view. Considering the reasons of saving economy, our experiment ultimately chose three proportions: 5%, 10%, and 20%.

Table S1 The elemental analysis of CYCU-3@ Al_2O_3(5、10、20、30 and 40%)

Name	N(%)	C(%)	H(%)	S(%)
CYCU-3@Al_2O_3(5%)	0.31	5.09	0.85	0.06
CYCU-3@Al_2O_3(10%)	0.37	5.86	0.91	0.05
CYCU-3@Al_2O_3(20%)	0.32	7.88	1.02	0.04
CYCU-3@Al_2O_3(30%)	0.34	7.93	1.02	0.05
CYCU-3@Al_2O_3(40%)	0.36	7.98	1.04	0.04

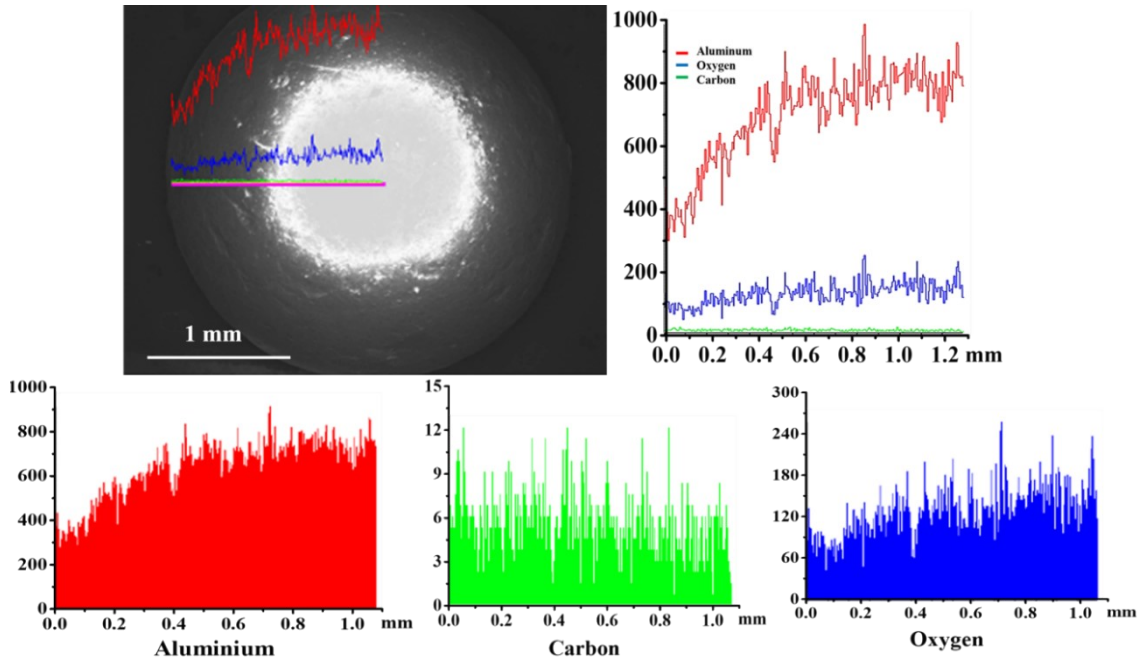

Fig. S1 Elemental lining of the cross-section of CYCU-3@Al_2O_3(20%) composite bead.

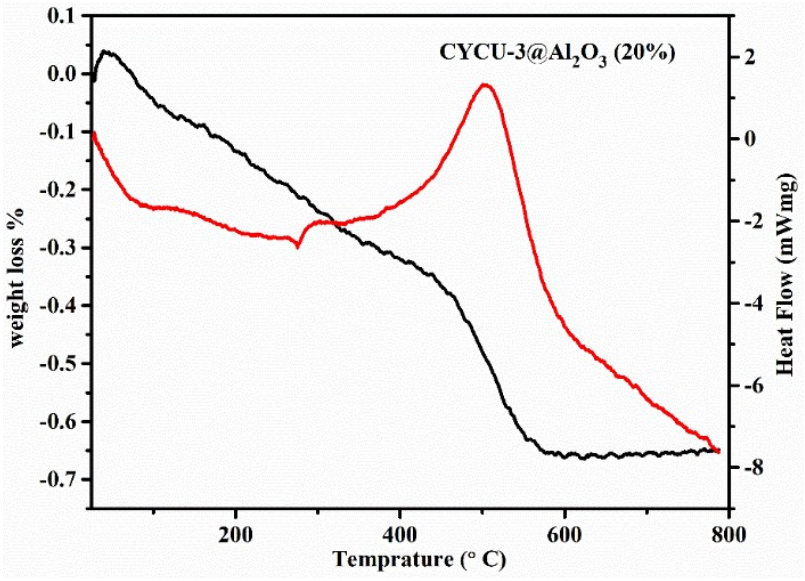

Fig. S2 TGA-DTA curves of the CYCU-3@Al_2O_3(20%) composite.

Table S2 BET surface area and pore size of CYCU-3@Al_2O_3 (5、10 and 20%) composites

	BET surface area (m^2/g)	DR method (0.35 – 10 nm)	BJH method (10 – 70 nm)
CYCU-3@Al_2O_3 (5%)	585	1.79	11.78
CYCU-3@Al_2O_3 (10%)	685	1.81	12.53
CYCU-3@Al_2O_3 (20%)	840	1.85	16.57

Table S3 The maximum adsorptive desulfurization capacities of DBT comparison between present work and some reported work.

Adsorbent	Q_{max} (mg S/g MOF)	Simulated oil	C_0 (ppmw_S) (System)
$Zn_4O(BDC)_3$[1]	12.7	iso-octane	300/fixed bed
$Zn_4O(BDC)_3$[1]	9.1	iso-oct:toluene(85:15)	300/fixed bed
MOF-505[1]	20.5	iso-octane	300/fixed bed
MOF-505[1]	14.9	iso-oct:toluene (85:15)	300/fixed bed

UMCM-150[1]	66.3	iso-octane	300/fixed bed
UMCM-150[1]	66.6	iso-oct:toluene (85:15)	300/fixed bed
MIL-101[2]	28.9	*n*-octane	~714/batch
ZIF-8-derived porous carbon [3]	26.7	*n*-hexane	<160/batch
ZIF-8-derived porous carbon [3]	22.2	*n*-hexane:para-xylene (9:1)	<174/batch
Cr-BDC[4]	41.0	*n*-octane	1000/batch
Cr-BTC[4]	30.7 This work	*n*-octane	1000/batch
Activated Al_2O_3[5]	21.0	*n*-hexane	<174/batch
CMK-3[6]	10.9	*n*-hexane	<261/batch
CMK-5[6]	21.7	*n*-hexane	<261/batch
Carbon aerogel[7]	15.1	*n*-hexadecane	<696/batch
Activated carbon[8]	28.9	*n*-octane	300/batch
Activated carbon spheres[9]	17.6	*n*-octane	<124/batch
Cu(I)-Y zeolite[10]	32.6	*n*-octane	~690/batch
Co-Y zeolite[10]	29.4	*n*-octane	~690/batch
Ce/Ni-Y zeolite[11]	22.2	*n*-octane	~124/batch
Activated Carbon loaded Na, Co, Ag or Cu[12]	65-115	*n*-hexane	178/batch
MC-Z(Cu, Co or Fe)[13]	51.4-75.5	*n*-hexane	178/batch
PT-Ag-MASN[14]	15.0[c]	*n*-decane	500/batch
HKUST-1[15]	59.6, 49.5	*n*-octane	1000/batch
HKUST-1@γ-Al_2O_3[16]	76.1, 59.7	*n*-octane	1000/batch
CYCU-3 This work	45.83	*n*-octane	1000/batch
CYCU-3@Al_2O_3(5%) This work	50.81	*n*-octane	1000/batch
CYCU-3@Al_2O_3(10%) This work	55.74	*n*-octane	1000/batch
CYCU-3@Al_2O_3(20%) This	62.3	*n*-octane	1000/batch

work

Table S4 Comparison of the adsorptive denitrogenation capacities of different adsorbents in model oil system.

Adsorbent	Type of NCCs	Q_e (mg-NCC/g)	Conditions	Reported
Activated Carbon[7, 17-19]	Quinoline, indole	-	39.0	--
Cu-Y[20]	NCCs with aromatic rings	-	3.0	--
Silica-zirconia cogel[21]	Mixed	-	10.0	--
Alumina[22]	Quinoline, indole	-	7.16	--
Uio-66-NH_2[23, 24]	IND	312	-	--
Uio-66-SO_3H[23, 24]	IND	239	-	--
MIL-101-ED[25]	IND	336	-	--
Uio-66-COOH[23, 24]	IND, PY	130	-	--
NH_2-Uio-66[23, 24]	indole	312	37.3	--
CYCU-3@Al_2O_3(20%)	indole	201	39	This work
	Quinoline	372	56	This work
	Acridine	393	63	This work

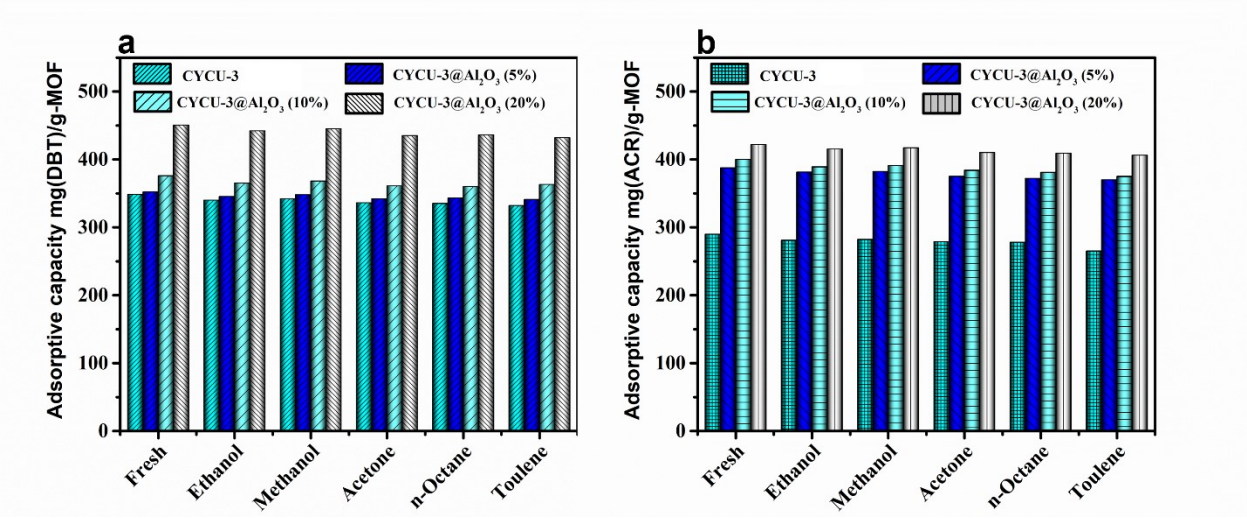

Fig. S3 Effect of solvents applied in the regeneration of the CYCU-3 and CYCU-3@γ-Al_2O_3 (5, 10 and 20%) composites on the adsorptive removal of DBT and ACR.

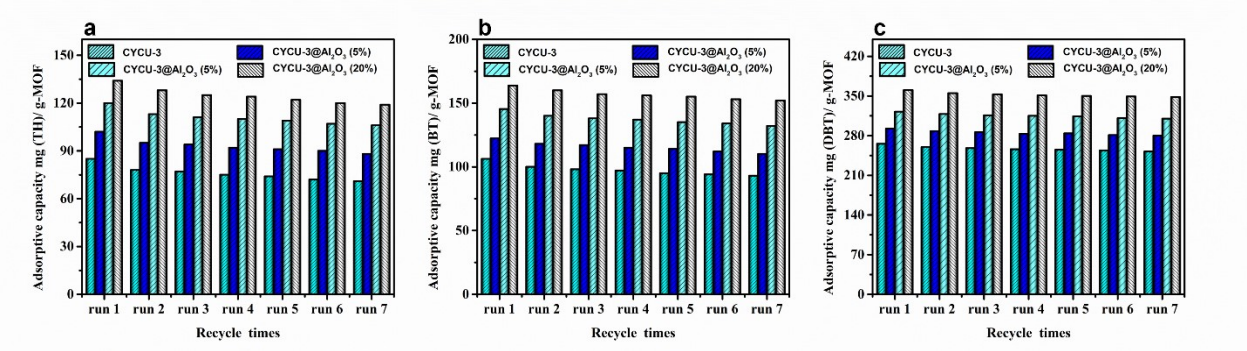

Fig. S4 Effect of regeneration cycles on the performances of adsorptive removal of TH, BT and DBT over regenerated CYCU-3 and CYCU-3@γ-Al_2O_3(5, 10 and 20%) composites (by washing with methanol). The recyclability experiments were carried in individual solution system. For every 10 mL of model fuel, 0.1g of adsorbent was applied.

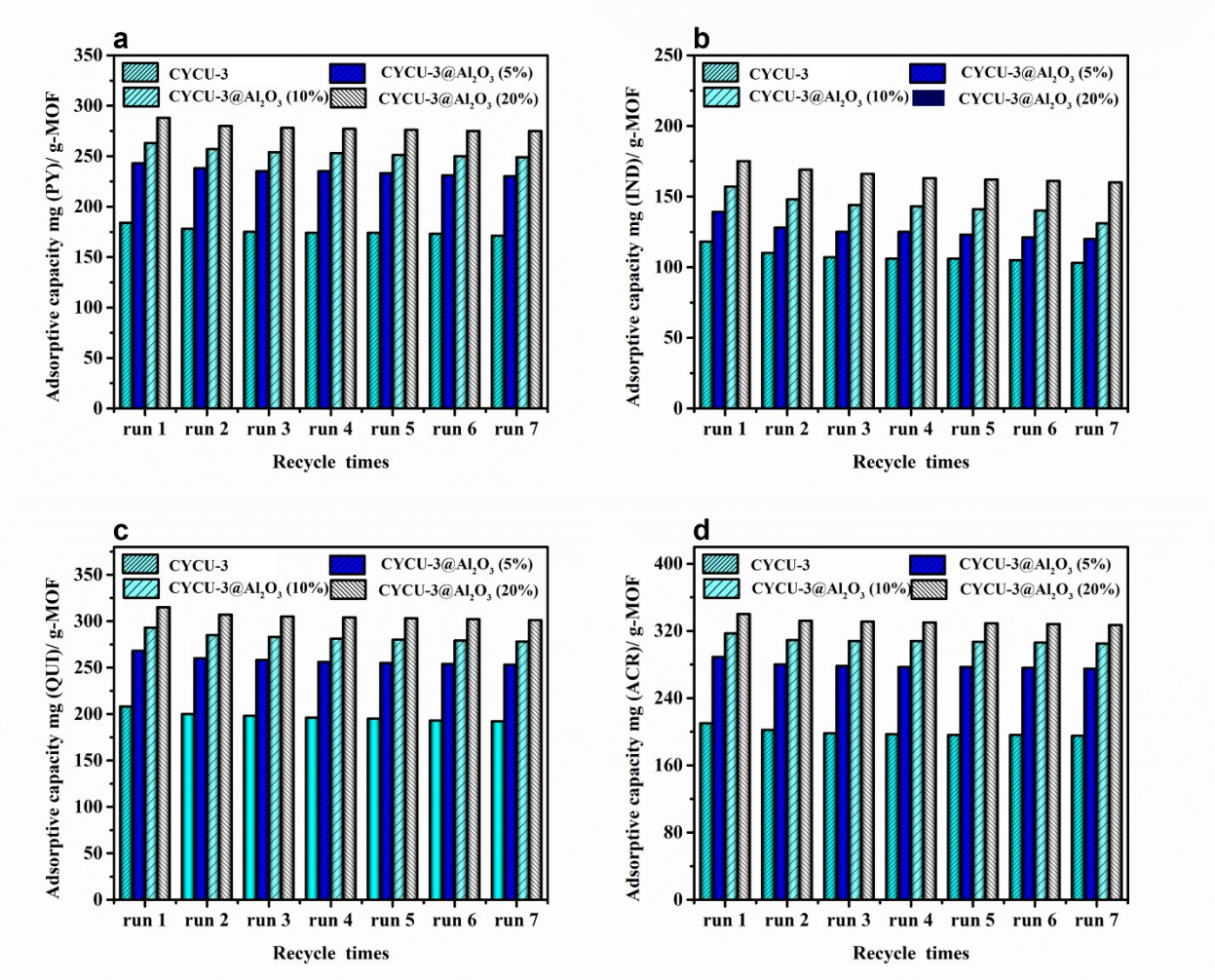

Fig. S5 Effect of regeneration cycles on the performances of adsorptive removal of PY, IND, QUI and ACR over regenerated CYCU-3 and CYCU-3@γ-Al_2O_3(5, 10 and 20%) composites (washing with methanol). The recyclability experiments were conceded in individual solution system. For every 10 mL of model fuel, 0.1 g of adsorbent was applied.

References

1. K. A. Cychosz, A. G. Wong-Foy and A. J. Matzger, *J. Am. Chem. Soc.*, 2009, **131**, 14538-14543.
2. M. Bagheri, M. Y. Masoomi and A. Morsali, *J. Hazard. Mater.*, 2017, **331**, 142-149.
3. Y. Shi, X. Zhang, L. Wang and G. Liu, *Alche. J.*, 2014, **60**, 2747-2751.
4. R.-H. Shi, Z.-R. Zhang, H.-L. Fan, T. Zhen, S. Ju and J. Mi, *Appl. Surf. Sci.*, 2017, **394**, 394-402.
5. A. Srivastav and V. C. Srivastava, *J. Hazard. Mater.*, 2009, **170**, 1133-1140.
6. E. Ghasemi, E. Alimardani, E. Shams and G. A. Koohmareh, *J. Electroanal. Chem.*, 2017, **789**, 92-99.
7. S. Haji and C. Erkey, *Ind. Eng. Chem. Res.*, 2003, **42**, 6933-6937.
8. Y. Shi, X. Zhang and G. Liu, *Fuel*, 2015, **158**, 565-571.
9. J. Qi, J. Li, Y. Li, X. Fang, X. Sun, J. Shen, W. Han and L. Wang, *Chem. Eng. J.*, 2017, **307**, 989-998.
10. H. Song, Y. Chang and H. Song, *Adsorption*, 2016, **22**, 139-150.
11. H. Song, G. Yang, H. Song, X. Cui, F. Li and D. Yuan, *J. Taiwan. Inst. Chem. E.*, 2016, **63**, 125-132.
12. C. O. Ania and T. J. Bandosz, *Carbon*, 2006, **44**, 2404-2412.
13. Z. X. Jiang, Y. Liu, X. P. Sun, F. P. Tian, F. X. Sun, C. H. Liang, W. S. You, C. R. Han and C. Li, *Langumir*,

2003, **19**, 731-736.
14. P. Tan, X.-Y. Xie, X.-Q. Liu, T. Pan, C. Gu, P.-F. Chen, J.-Y. Zhou, Y. Pan and L.-B. Sun, *J. Hazard. Mater.*, 2017, **321**, 344-352.
15. L. Qin, Y. Zheng, D. Li, Y. Zhou, L. Zhang and Z. Zuhra, *Fuel*, 2016, **181**, 827-835.
16. L. Qin, Y. Zhou, D. Li, L. Zhang, Z. Zhao, Z. Zuhra and C. Mu, *Ind. Eng. Chem. Res.*, 2016, **55**, 7249-7258.
17. B. K. Jung and S. H. Jhung, *Fuel*, 2015, **145**, 249-255.
18. N. A. Khan, Z. Hasan, K. S. Min, S.-M. Paek and S. H. Jhung, *Fuel. Process. Technol.*, 2013, **116**, 265-270.
19. X. Han, H. Lin and Y. Zheng, *Can. J. Chem. Eng.*, 2015, **93**, 538-548.
20. A. J. Hernandez-Maldonado and R. T. Yang, *Alche. J.*, 2004, **50**, 791-801.
21. Y. S. Bae, M. B. Kim, H. J. Lee, C. H. Lee and J. W. Ryu, *Alche. J.*, 2006, **52**, 510-521.
22. H. Zhang, G. Shan, H. Liu and J. Xing, *Surf. Coat. Tech.*, 2007, **201**, 6917-6921.
23. I. Ahmed, N. A. Khan and S. H. Jhung, *Chem. Eng. J.*, 2017, **321**, 40-47.
24. M. Sarker, H. J. An and S. H. Jhung, *J. Phys. Chem. C.*, 2018, **122**, 4532-4539.
25. P. W. Seo, I. Ahmed and S. H. Jhung, *Phys. Chem. Chem. Phys.*, 2016, **18**, 14787-14794.